Fluctuating hydrodynamics and correlation lengths in a driven granular fluid

G Gradenigo, A Sarracino, D Villamaina and A Puglisi

CNR-ISC and Dipartimento di Fisica, Università Sapienza—Piazzale Aldo Moro 2, Roma 00185, Italy

E-mail: ggradenigo@gmail.com, alessandro.sarracino@roma1.infn.it, dario.villamaina@roma1.infn.it and andrea.puglisi@roma1.infn.it

Abstract. Static and dynamical structure factors for shear and longitudinal modes of the velocity and density fields are computed for a granular system fluidized by a stochastic bath with friction. Analytical expressions are obtained through fluctuating hydrodynamics and are successfully compared with numerical simulations up to a volume fraction ~50%. The hydrodynamic noise is the sum of the external noise due to the bath and the internal one due to collisions. Only the latter is assumed to satisfy the fluctuation-dissipation relation with the average granular temperature.

The static velocity structure factors $S_\perp(k)$ and $S_\parallel(k)$ display a general non-constant behavior with two plateaux at large and small k, representing the granular temperature T_g and the bath temperature $T_b > T_g$ respectively. From this behavior, two different velocity correlation lengths are measured, both increasing as the packing fraction is raised. This growth of spatial order is in agreement with the behavior of dynamical structure factors, the decay of which becomes slower and slower at increasing density.

J. Stat. Mech. (2011) P08017

Contents

1. Introduction

Granular media display a wide catalog of non-equilibrium phenomena [1]. These materials are constituted of a number N of elementary constituents, grains of typical diameter between 0.1 and 10 mm. The number $N \gg 1$ is usually large enough to allow, or require, a statistical treatment. Unfortunately, the interactions are non-conservative, resulting in the failure of equilibrium statistical mechanics. Kinetic theories, from the Boltzmann equation to hydrodynamics [2], together with numerical simulations [3], are the best tools to describe these systems and to compare with real experiments, with the caveat of a proper adaptation to the peculiarity of granular interactions.

One of the debated points of granular kinetic theories is the way in which noise should be added to the hydrodynamics in order to describe mesoscopic fluctuations [4, 5]. This is a general problem in non-equilibrium systems [6] (e.g. sheared fluids [7]), but here is even more pressing, given the rather small number of particles in a granular system: one has typically $N \sim 10^3$–10^4, even in experiments, so that fluctuations can hardly be neglected. Moreover, in granular systems the dynamics is non-conservative and therefore fluctuation-dissipation relations do not hold in general [8]–[11], with exceptions in driven dilute cases [12]–[14]. In non-dilute systems, it is therefore difficult even to define a temperature, making the modelization of fluctuations tricky [15, 16].

A comprehensive study of the fluctuating hydrodynamics of a driven granular fluid is presented here. Static and dynamical structure factors are computed analytically in the framework of linearized hydrodynamics, and compared with extensive numerical

simulations. A very good agreement is found between the analytical and numerical results in a wide range of parameters, implying that, for this kind of model, fluctuating hydrodynamics is able to describe large-scale fluctuations in a satisfactory manner.

The peculiarity of the model we have studied, when compared to others present in the literature [17, 18], is the prescription for the stochastic bath used to keep the system at stationarity. In particular, our thermostat is able to equilibrate the system also when collisions are elastic [19]. This happens because, in addition to a random driving, our thermostat acts on the particles also through a finite drag, in such a way that the temperature of the thermostat $T_{\rm b}$, different from the kinetic temperature of the fluid $T_{\rm g} < T_{\rm b}$, is always well defined.

A remarkable feature of our model, related to the kind of thermostat we use, is the finite extent of velocity correlations in space. Indeed, the characteristic shape we find for transverse and longitudinal velocity structure factors allows us to define two non-equilibrium correlation lengths, ξ and $\xi_{\rm l}$, which are known functions of the kinematic and longitudinal viscosities, respectively. This means that, instead of sampling trajectories of the system, out of equilibrium an average of static observables is enough to measure transport coefficients. The flattening of the velocity structure factors at equilibrium clearly results in our formulas from the vanishing of the amplitude of the velocity correlations, which is proportional to $T_{\rm b} - T_{\rm g}$. In that case, access to transport coefficients is only possible through the study of the dynamical structure factors.

Finally, we study the behavior of such coherence lengths at different packing fractions. We observe a significant growth of the relative extent of the correlations ξ/λ_0 and $\xi_{\rm l}/\lambda_0$ with the packing fraction, where λ_0 denotes the mean free path. This is in agreement with the slowing down of the dynamics also observed in dense granular fluids [20].

This paper is organized as follows. In section 2 we discuss the model, the corresponding hydrodynamic equations and the specific forms of noise used. The k dependence of the eigenvalues of the linearized hydrodynamic matrix is also studied in order to check the stability and bounds of the linear approximation. In section 3 we present a complete study of the static and dynamical structure factors for the velocity and density modes, comparing analytical predictions and numerical results. In section 4 a discussion about the main findings is presented, with conclusions and perspectives for future work. In appendix A and appendix B we report, respectively, formulas for the transport coefficients and some details on the noise terms.

2. Microscopic model and fluctuating hydrodynamics

We consider a system of N inelastic hard spheres in d dimensions with mass m and diameter σ. The particles are contained in a volume $V = L^d$, with L the linear size of the system. We denote by $n = N/V$ the number density and by ϕ the occupied volume fraction (in two dimensions $\phi = N\pi(\sigma/2)^2/V$). The particles undergo binary instantaneous inelastic collisions when coming into contact, with the following rule:

$$\mathbf{v}_i = \mathbf{v}'_i - \frac{(1+\alpha)}{2}[(\mathbf{v}'_i - \mathbf{v}'_j) \cdot \hat{\boldsymbol{\sigma}}]\hat{\boldsymbol{\sigma}}, \tag{1}$$

where $\mathbf{v}_i$ ($\mathbf{v}_j$) and $\mathbf{v}'_i$ ($\mathbf{v}'_j$) are the post- and pre-collisional velocities of particle i (particle j), respectively; $\alpha \in [0, 1]$ is the restitution coefficient (in the elastic case $\alpha = 1$), and $\hat{\boldsymbol{\sigma}}$ is the unit vector joining the centers of the colliding particles.

In order to maintain a stationary fluidized state, an external energy source is coupled to every particle in the form of a thermal bath [19]. In particular, the motion of a particle i with velocity $\mathbf{v}_i$ is described by the following stochastic equation:

$$m\dot{\mathbf{v}}_i(t) = -\gamma_{\mathrm{b}}\mathbf{v}_i(t) + \boldsymbol{\xi}_{\mathrm{b},i}(t) + \mathbf{F}_i. \tag{2}$$

Here γ_{b} is a drag coefficient (which defines the characteristic interaction time with the external bath, $\tau_{\mathrm{b}}^{-1} = \gamma_{\mathrm{b}}/m$), $\boldsymbol{\xi}_{\mathrm{b},i}(t)$ is a white noise with $\langle \boldsymbol{\xi}_{\mathrm{b},i}(t) \rangle = 0$ and $\langle \xi_{\mathrm{b},i\alpha}(t)\xi_{\mathrm{b},j\beta}(t') \rangle = 2T_{\mathrm{b}}\gamma_{\mathrm{b}}\delta_{ij}\delta_{\alpha\beta}\delta(t-t')$ (Greek indices denote Cartesian coordinates), while $\mathbf{F}_i$ represents the action of particle–particle inelastic collisions. The effect of the external energy source balances the energy lost in the collisions so that an out-of-equilibrium stationary state is attained [19]. In particular, let us stress that such an energy injection mechanism acts homogeneously across the whole system, differently from other mechanisms where the energy is directly supplied only to a part of the system, as for instance for fluids under shear, or for systems in contact with vibrating walls.

The stationary state is characterized by two time-scales and two energy scales: the time-scales are τ_{b} and the mean free time between collisions τ_{c}; the energy scales are the temperature of the thermostat T_{b} and the granular temperature $T_{\mathrm{g}} = \sum_{i=1}^{N} m\langle v_i^2 \rangle/dN \leq T_{\mathrm{b}}$ (the equals sign holds only if $\alpha = 1$ or if $\tau_{\mathrm{b}} \ll \tau_{\mathrm{c}}$). In particular, in the dilute limit, the granular temperature T_{g} satisfies the following equation in the non-equilibrium stationary state [14]:

$$T_{\mathrm{g}} = T_{\mathrm{b}} - A_{\mathrm{d}}\frac{\chi(\phi)\phi(1-\alpha^2)}{2\gamma_{\mathrm{b}}}T_{\mathrm{g}}^{3/2}, \tag{3}$$

where $A_{\mathrm{d}} = \sqrt{m/\pi}2^{d-1}d/\sigma$ and $\chi(\phi)$ is the pair correlation function at contact. The model has a well-defined elastic limit $\alpha \to 1$, where the fluid equilibrates to the bath temperature, $T_{\mathrm{g}} = T_{\mathrm{b}}$. The viscous drag term $-\gamma_{\mathrm{b}}\mathbf{v}_i$ in equation (2) models the interaction between each particle and the thermostat. It is important to observe that γ_{b} is not related to the transport coefficients of the granular fluid and is fixed as a model parameter. As mentioned above, γ_{b} introduces a time-scale τ_{b} in the system that rules the tendency of a particle to relax toward equilibrium at temperature T_{b}. The characteristic time of collisions, τ_{c}, in all our simulations will be kept much smaller than τ_{b}; for this reason τ_{c} is considered the microscopic time-scale of our system since it dictates the smallest scale of relaxation toward the non-equilibrium stationary state. In particular, in the coarse-grained hydrodynamic description to be introduced below, we will take care of comparing the characteristic decay times of different hydrodynamic modes with τ_{c}, to verify the presence of a sufficient separation of scales.

In the following we will present a thorough numerical analysis of model (2), using an event-driven molecular dynamics algorithm [21]. In particular, we will consider periodic boundary conditions in $d = 2$ dimensions. The fixed parameters of the simulations are $m = 1$, $\sigma = 0.01$, $T_{\mathrm{b}} = 1$ and $\gamma_{\mathrm{b}} = 1$. The packing fraction is varied by changing the seize of the box, and we consider systems with $\phi \in [0.1, 0.5]$. The simulation data on static structure factors are obtained for a system of $N = 10\,000$ particles, averaged over about 100 realizations, whereas the results on dynamical correlators are obtained with samples of $N = 1000$ particles, averaged over about 4000 realizations.

2.1. Linearized hydrodynamics

Because we are interested in the behavior of large-scale spatial correlations in our system, we introduce here the coarse-grained hydrodynamic fields $n(\mathbf{r}, t), \mathbf{u}(\mathbf{r}, t)$ and $T(\mathbf{r}, t)$ as follows:

$$n(\mathbf{r}, t) = \sum_i \delta(\mathbf{r} - \mathbf{r}_i(t)), \qquad \mathbf{u}(\mathbf{r}, t) = \frac{1}{n} \sum_i \mathbf{v}_i(t) \delta(\mathbf{r} - \mathbf{r}_i(t)),$$
$$T(\mathbf{r}, t) = \frac{2m}{dn} \sum_i \frac{v_i^2(t)}{2} \delta(\mathbf{r} - \mathbf{r}_i(t)). \tag{4}$$

The hydrodynamic equations for the fields (4) can be derived for the model (2) following a standard recipe [22]–[24]:

$$\partial_t n(\mathbf{r}, t) = -\boldsymbol{\nabla} \cdot (n(\mathbf{r}, t) \mathbf{u}(\mathbf{r}, t)),$$
$$\partial_t \mathbf{u}(\mathbf{r}, t) + \mathbf{u} \cdot \boldsymbol{\nabla} \mathbf{u} = -\frac{1}{\rho} \boldsymbol{\nabla} \cdot \boldsymbol{\Pi} - \frac{\gamma_b}{m} \mathbf{u}(\mathbf{r}, t), \tag{5}$$
$$\partial_t T(\mathbf{r}, t) + \mathbf{u} \cdot \boldsymbol{\nabla} T = -\frac{2}{nd}(\boldsymbol{\nabla} \cdot \mathbf{J} + \boldsymbol{\Pi} : \boldsymbol{\nabla} \mathbf{u}) - \Gamma + 2\frac{\gamma_b}{m}(T_b - T(\mathbf{r}, t)).$$

In the above equations $\mathbf{J}$ and $\boldsymbol{\Pi}$ are respectively the heat flux and the pressure tensor, see details in appendix B, and $\gamma_0 = (1 - \alpha^2)/2d$. In the velocity equation the viscous drag term $-\gamma_b \mathbf{u}/m$ has been inserted, while in the temperature equation three terms have been added: the sink term $-\Gamma = -2\gamma_0 \omega_c T(\mathbf{r}, t)$ [25], where $\omega_c \sim \sqrt{T(\mathbf{r}, t)}$ is the collision frequency, takes into account the energy dissipated by inelastic collisions, while the terms $2\gamma_b(T_b - T)/m$ represent the energy exchanged with the thermostat.

Equations (5) give a fair description of the mesoscopic degrees of freedom of a granular fluid as long as a proper separation of space and time-scales is verified between those degrees of freedom and all the microscopic ones which are projected out. This condition is, of course, not always satisfied [26]–[28], but is not prevented in principle and is, indeed, realized in many experiments or simulations [29]–[31], [20, 32].

Equations (5) can be linearized around the stationary homogeneous state, where the hydrodynamic fields take the values $n = \bar{n}$, $T = \bar{T}$ and $\mathbf{u} = 0$. A system of linear differential equations for the fluctuations $\delta \mathbf{a}(\mathbf{k}, t) = \{\delta n(\mathbf{k}, t), \delta T(\mathbf{k}, t), u_\parallel(\mathbf{k}, t), u_\perp(\mathbf{k}, t)\}$, with $\delta a = a - \bar{a}$, can be considered, with the Fourier transform defined as

$$\delta \mathbf{a}(\mathbf{k}, t) = \int \mathrm{d}\mathbf{r}\, \delta \mathbf{a}(\mathbf{r}, t) \mathrm{e}^{-\mathrm{i}\mathbf{k} \cdot \mathbf{r}}, \tag{6}$$

and with $u_\perp(\mathbf{k}, t)$ and $u_\parallel(\mathbf{k}, t)$ respectively the shear and longitudinal modes, namely

$$u_\parallel(\mathbf{k}) = \hat{k} \cdot \mathbf{u}(\mathbf{k}) \qquad u_\perp(\mathbf{k}) = \hat{k}_\perp \cdot \mathbf{u}(\mathbf{k}), \tag{7}$$

$\hat{k}_\perp$ being a unitary vector such that $\hat{k}_\perp \cdot \hat{k} = 0$. The system in equation (5) in Fourier space becomes

$$\delta \dot{\mathbf{a}}(\mathbf{k}, t) = \mathbf{M}(k) \delta \mathbf{a}(\mathbf{k}, t), \tag{8}$$
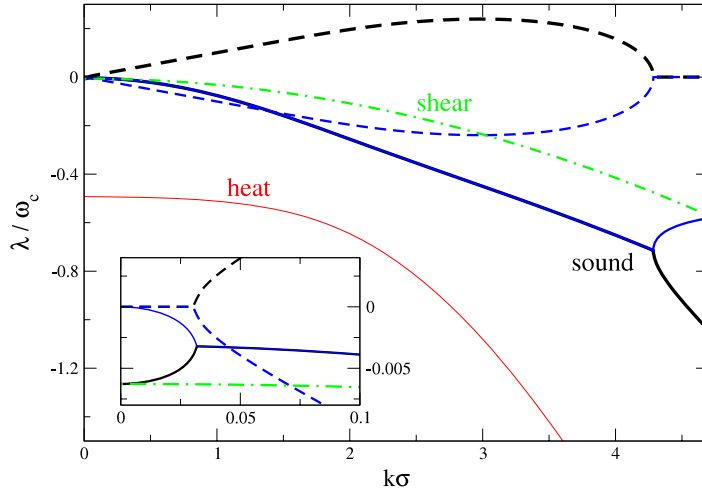
Figure 1. Eigenvalue spectrum $\lambda(k)$ of the dynamical matrix (9) calculated for $\phi = 0.5$ and $\alpha = 0.6$, namely in a strongly inelastic regime. The eigenvalues are normalized on the Enskog collision frequency ω_c so that on the y axis the ratio $\tau_c/\tau(k) = \lambda(k)/\omega_c$ between the microscopic time-scale of the model and the decay time of each mode can be directly read. Inset: zoom of the spectrum at small k.

with the dynamical matrix

$$
\mathbf{M}(k) = - \begin{pmatrix}
0 & 0 & ikn & 0 \\
\gamma_0 \omega_c g(n) T_g/n & 3\gamma_0 \omega_c + D_T k^2 + 2\gamma_b/m & i2kp/dn & 0 \\
ikv_T^2/n & ikp/\rho T_g & \nu_l k^2 + \gamma_b/m & 0 \\
0 & 0 & 0 & \nu k^2 + \gamma_b/m
\end{pmatrix}, \quad (9)
$$

where $\rho = nm$, $D_T = 2\kappa/nd$ is the thermal diffusion coefficient (κ is the heat conductivity), while ν and ν_l are the kinematic and longitudinal viscosity respectively. Formulas for all parameters and transport coefficients are given in appendix A. There we refer to the Enskog theory for dense elastic hard spheres (EHS) [33], which provides a good approximation, as observed in [18, 34]. The following sections are devoted to showing how the viscosities ν and ν_l can be obtained as fitting parameters of static and dynamical correlations. Such results will be compared with the dense EHS predictions, finding good agreement.

2.2. Spectrum of the hydrodynamic matrix and separation of time-scales

We analyze the eigenvalues of $\mathbf{M}(k)$ in order to study the linear stability of the model and to characterize the range of validity of time-scale separation required by hydrodynamics. From the expression in equation (9) we learn that the shear modes are decoupled from all the others, and the typical time-scale of their decay simply reads as $\tau_\perp = (\gamma_b/m + \nu k^2)^{-1}$. To obtain the typical time-scales for the fluctuations of the other hydrodynamic fields we solve, numerically, the equation $\text{Det}(\mathbf{M}(k) - \lambda(k)\mathbf{I}) = 0$, where $\mathbf{I}$ is the identity matrix. The eigenvalue spectrum thus found is shown in figure 1, for parameters of the model $\alpha = 0.6$ and $\phi = 0.5$. All parameters are calculated according to the formulas reported in appendix A.

The study of hydrodynamic eigenvalues shows that, even in the case of a quite inelastic and dense regime, a range of scales where the mesoscopic relaxation times are larger than the microscopic times exists and a hydrodynamic description can be attempted. In particular, comparing the eigenvalues $\lambda_i(k)$ with the Enskog frequency ω_c (which will be verified, below, to be a good estimate of the real frequency in simulations), see figure 1, we find, for each eigenvalue, the interval of values of k where $\lambda_i/\omega_c < 1$ is fulfilled. The subscript i indicates eigenvalues related to heat ($i = H$), sound ($i = \pm$) and shear ($i = \perp$) modes. The range is narrower for the case of the mode dominated by temperature fluctuations (denoted 'heat mode' in the figure, red thin curve), while it is larger for shear modes (green dot-dashed lines) and modes dominated by longitudinal velocities and density fluctuations (here referred to as 'sound modes', black and blue thick curves, continuous for the real part and dashed for the imaginary part).

A general observation is that the eigenvalues never have a positive real part, i.e. no instabilities are found, thanks to the presence of the external bath. Moreover, for the whole range of k studied, the two 'sound modes'—as usual—are complex conjugate, i.e. they propagate with a k-dependent velocity. A negative real part is always present, determining overall damping. At small values of k one can identify a sound velocity c by observing a linear relation $\mathrm{Im}[\lambda_\pm] \sim ck$; instead the dispersion relation becomes strongly nonlinear at large k. Surprisingly, the study of sound eigenvalues shows that they have bifurcations at very small $k < k_1$ and very large $k > k_2$ wavenumbers, becoming in both limits pure real numbers, i.e. losing their propagating behavior. Those bifurcations are due to the external damping, ruled by γ_b; indeed in the limit $\gamma_b \to 0$ (keeping finite $\gamma_b T_b$), they disappear and the spectrum studied in [18, 20] is retrieved. Moreover, we find that the wavevector k_1 where the first bifurcation occurs moves toward smaller values of k when the dissipation is increased, namely when α is decreased (at fixed ϕ) or when ϕ is increased (at fixed α). Looking closely at the bifurcations, we see that one of the eigenvalues for 'sound modes' approaches 0 for $k \to 0$ (representing total number conservation) and the other tends to $-\gamma_b/m$ (as the shear one), see the inset of figure 1. The bifurcation at large k is perhaps non-physical, as it always falls out of the hydrodynamic range. For the eigenvalue of the heat mode we find that $\lambda_H(k = 0) = -(3\gamma_0\omega_c + 2\gamma_b/m)$. In the numerical setup used below, we have $k_{\min} = 2\pi/L > k_1$, so that the purely exponential decay of sound modes with large waves is never observed.

2.3. Stochastic description with fluctuating hydrodynamics

In order to fully account for the spatial fluctuations of the hydrodynamic fields and for the decay in time of such fluctuations we must add some noise terms to the linearized hydrodynamic equations: the basic assumption under fluctuating hydrodynamics is the same as for average (deterministic) hydrodynamics, i.e. a good separation of scales between hydrodynamic fields and microscopic degrees of freedom. In the linearized hydrodynamic equations the small-scale fluctuations have been projected out, but their feedback on large-scale fluctuations can be recovered by a proper addition of noise terms to the dynamical equations:

$$\delta\dot{\mathbf{a}}(\mathbf{k}, t) = \mathbf{M}(k)\delta\mathbf{a}(\mathbf{k}, t) + \mathbf{f}(\mathbf{k}, t). \tag{10}$$

A derivation from first principles of the noise $\mathbf{f}(\mathbf{k}, t)$ is beyond our scope. A kinetic theory with fluctuations has been recently proposed in [35, 36], for the homogeneous

cooling regime, which is very different from our case. A similar treatment has been realized, only for the shear mode, in a driven case (random kicks without damping, i.e. $\gamma_b = 0$) [37], showing that noise can be safely assumed to be white, differently from the cooling regime. In such a case, with an additional but reasonable assumption on the two-particle velocity autocorrelation functions (namely, that such functions only have components in the hydrodynamic subspace), it is found that the fluctuation–dissipation relation for the internal part of the noise is satisfied, as already assumed in [25, 18]. Following those previous studies, we will consider such an assumption valid. Notice that it does not imply that fluctuation–dissipation relations will be satisfied by the whole noise, which is composed of internal as well as external contributions. In summary we write

$$
\mathbf{f}(\mathbf{k}, t) = \begin{pmatrix} 0 \\ \theta^{\mathrm{ex}}(\mathbf{k}, t) + 2\mathrm{i}k/nd \; \theta^{\mathrm{in}}(\mathbf{k}, t) \\ \xi_{\mathrm{l}}^{\mathrm{ex}}(\mathbf{k}, t) + \mathrm{i}k/\rho \; \xi_{\mathrm{l}}^{\mathrm{in}}(\mathbf{k}, t) \\ \xi_{\perp}^{\mathrm{ex}}(\mathbf{k}, t) + \mathrm{i}k/\rho \; \xi_{\perp}^{\mathrm{in}}(\mathbf{k}, t) \end{pmatrix},
\tag{11}
$$

where the two sources of noise for the hydrodynamic field fluctuations are put in evidence: the first is the external contribution coming directly from the thermal bath, namely the stochastic force $\boldsymbol{\xi}_b$ of equation (2); the second is internal and enters through the constitutive equations for the heat flux and the pressure tensor. A detailed discussion on noises is presented in appendix B. The external and internal noises are Gaussian with zero average. The variances of external noises can be obtained directly from equations (2) and (4):

$$
\langle \theta^{\mathrm{ex}}(\mathbf{k}, t) \theta^{\mathrm{ex}}(\mathbf{k}', t') \rangle = \frac{4mT_g}{dn} \frac{2\gamma_b T_b}{m} \delta(t - t') \delta(\mathbf{k} + \mathbf{k}'),
$$
$$
\langle \xi_{\mathrm{l}}^{\mathrm{ex}}(\mathbf{k}, t) \xi_{\mathrm{l}}^{\mathrm{ex}}(\mathbf{k}', t') \rangle = \langle \xi_{\perp}^{\mathrm{ex}}(\mathbf{k}, t) \xi_{\perp}^{\mathrm{ex}}(\mathbf{k}', t') \rangle = \frac{1}{n} \frac{2\gamma_b T_b}{m} \delta(t - t') \delta(\mathbf{k} + \mathbf{k}'),
\tag{12}
$$

while the variances of the internal contributions are obtained by imposing the fluctuation–dissipation theorem (see appendix B for details):

$$
\langle \theta^{\mathrm{in}}(\mathbf{k}, t) \theta^{\mathrm{in}}(\mathbf{k}', t') \rangle = 2\kappa T_g^2 \delta(t - t') \delta(\mathbf{k} + \mathbf{k}'),
$$
$$
\langle \xi_{\mathrm{l}}^{\mathrm{in}}(\mathbf{k}, t) \xi_{\mathrm{l}}^{\mathrm{in}}(\mathbf{k}', t') \rangle = 2nm\nu_1 T_g \delta(t - t') \delta(\mathbf{k} + \mathbf{k}'),
$$
$$
\langle \xi_{\perp}^{\mathrm{in}}(\mathbf{k}, t) \xi_{\perp}^{\mathrm{in}}(\mathbf{k}', t') \rangle = 2nm\nu T_g \delta(t - t') \delta(\mathbf{k} + \mathbf{k}').
\tag{13}
$$

The internal and external noises are uncorrelated:
$$
\langle \theta^{\mathrm{ex}}(\mathbf{k}, t) \theta^{\mathrm{in}}(\mathbf{k}', t') \rangle = \langle \xi_{\mathrm{l}}^{\mathrm{ex}}(\mathbf{k}, t) \xi_{\mathrm{l}}^{\mathrm{in}}(\mathbf{k}', t') \rangle = \langle \xi_{\perp}^{\mathrm{ex}}(\mathbf{k}, t) \xi_{\perp}^{\mathrm{in}}(\mathbf{k}', t') \rangle = 0.
\tag{14}
$$

The hydrodynamic analysis of model (2) consists, then, in solving the system of coupled linear Langevin equations (10). In particular, we are interested in finding the explicit forms of the static and dynamical structure factors, respectively,

$$
S_{ab}(\mathbf{k}) = \lim_{t \to \infty} \frac{1}{V} \langle \delta a(\mathbf{k}, t) \delta b(-\mathbf{k}, t) \rangle,
\tag{15}
$$

and

$$
S_{ab}(\mathbf{k}, \omega) = \int_{-\infty}^{\infty} S_{ab}(\mathbf{k}, t) \mathrm{e}^{-\mathrm{i}\omega t},
\tag{16}
$$

where

$$
S_{ab}(\mathbf{k}, t) = \lim_{t' \to \infty} \frac{1}{V} \langle \delta a(\mathbf{k}, t' + t) \delta b(-\mathbf{k}, t') \rangle.
\tag{17}
$$

3. Out-of-equilibrium correlations: static and dynamical structure factors

It is well known that spatially extended correlations develop in the non-equilibrium stationary state of a driven granular fluid [18, 20]. In particular, the velocity correlator $\langle \mathbf{u}(\mathbf{k}) \cdot \mathbf{u}(-\mathbf{k}) \rangle$, where the average $\langle \cdots \rangle$ is taken over noises, can be written as

$$\langle \mathbf{u}(\mathbf{k}) \cdot \mathbf{u}(-\mathbf{k}) \rangle = \langle u_\parallel(\mathbf{k}) u_\parallel(-\mathbf{k}) \rangle + \langle u_\perp(\mathbf{k}) u_\perp(-\mathbf{k}) \rangle, \tag{18}$$

with the cross terms $\langle u_\perp(\mathbf{k}) u_\parallel(-\mathbf{k}) \rangle = 0$. The two terms on the right of equation (18) can be studied separately.

3.1. Shear modes

According to the matrix (9) the shear modes are decoupled from the others in the linear approximation and their dynamics obeys a simple Langevin equation

$$\dot{u}_\perp(\mathbf{k}, t) = -(\gamma_{\mathrm{b}} + \nu k^2) u_\perp(\mathbf{k}, t) + \xi_\perp^{\mathrm{ex}}(\mathbf{k}, t) + \mathrm{i} k/n \xi_\perp^{\mathrm{in}}(\mathbf{k}, t), \tag{19}$$

where, from now on, we put $m = 1$ in all formulas. The effect of internal and external noises is equal to a single complex noise $\xi_\perp(\mathbf{k}, t) = \xi_\perp^{\mathrm{ex}}(\mathbf{k}, t) + \mathrm{i} k/n \xi_\perp^{\mathrm{in}}(\mathbf{k}, t)$ with variance

$$V^{-1} \langle \xi_\perp(\mathbf{k}, t) \xi_\perp(-\mathbf{k}, t') \rangle = \frac{2}{n} (T_{\mathrm{b}} \gamma_{\mathrm{b}} + \nu T_{\mathrm{g}} k^2) \delta(t - t'). \tag{20}$$

From this, the equal-time correlator $\langle u_\perp(\mathbf{k}) u_\perp(-\mathbf{k}) \rangle$ can be easily calculated:

$$n S_\perp(k) = N^{-1} \langle |u_\perp(k)|^2 \rangle = \frac{\gamma_{\mathrm{b}} T_{\mathrm{b}} + \nu k^2 T_{\mathrm{g}}}{\gamma_{\mathrm{b}} + \nu k^2} = T_{\mathrm{g}} + \frac{(T_{\mathrm{b}} - T_{\mathrm{g}})}{1 + \xi^2 k^2}, \tag{21}$$

with $\xi^2 = \nu/\gamma_{\mathrm{b}}$. The meaning of the above equation is clear: the small length-scale physics, which depends on the inelastic collisions, is related to the granular temperature T_{g}, while at large distances there are correlations with finite amplitude $T_{\mathrm{b}} - T_{\mathrm{g}}$ and extent ξ. Notice that in the limit $\gamma_{\mathrm{b}} \to 0$, keeping $\gamma_{\mathrm{b}} T_{\mathrm{b}}$ finite, from equation (21) one obtains the result of [18], where $S_\perp(k) \sim 1/k^2$ and long range correlations are observed. A similar power law behavior is also observed in molecular fluids under shear [7]. The different result we obtain in our model is due to the intrinsic cut-off introduced by the viscous drag $\gamma_{\mathrm{b}} > 0$. Indeed, the finite extent of the correlations is even clearer when equation (21) is written in real space, yielding the spatial correlation function $G_\perp(\mathbf{r})$, which reads

$$n G_\perp(\mathbf{r}) = T_{\mathrm{g}} \delta^{(2)}(\mathbf{r}) + (T_{\mathrm{b}} - T_{\mathrm{g}}) \frac{K_0(r/\xi)}{\xi^2}, \tag{22}$$

where $K_0(x)$ is the second kind modified Bessel function that, for large distances, decays exponentially

$$K_0(r/\xi) \approx \sqrt{\frac{\pi}{2}} \frac{\mathrm{e}^{-r/\xi}}{(r/\xi)^{1/2}}. \tag{23}$$

At equilibrium, namely when the collisions are elastic and $T_{\mathrm{g}} = T_{\mathrm{b}}$, equipartition between modes is perfectly fulfilled and the structure factor becomes flat, i.e. $S_\perp(k) = T_{\mathrm{b}}$. Differently, in the granular case, where $T_{\mathrm{g}} \neq T_{\mathrm{b}}$, equipartition breaks down and from equation (21) we have that $S_\perp \to T_{\mathrm{b}}$ for small k and $S_\perp \to T_{\mathrm{g}}$ for large k. We see here that out of equilibrium the quantity $\xi = \sqrt{\nu/\gamma_{\mathrm{b}}}$ measures the range of static correlations of
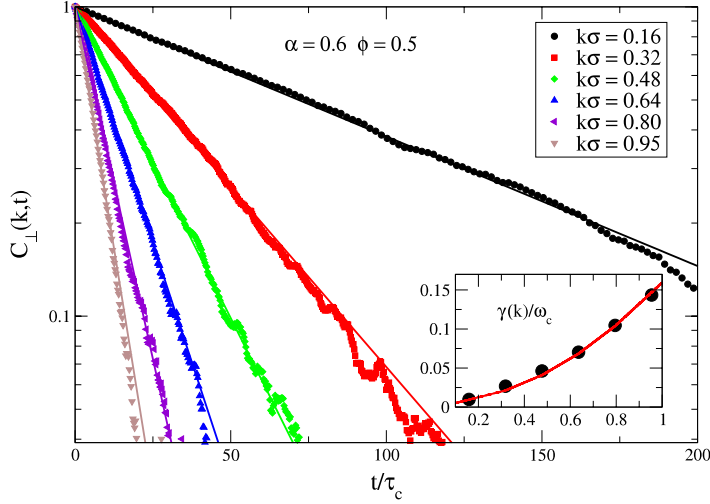
Figure 2. $C_\perp(k,t)$ for $\alpha = 0.6$ and $\phi = 0.5$ and several values of $k\sigma$ measured in numerical simulations, together with exponential fits (continuous curves). In the inset the quantity $\gamma(k)$ obtained from the fits is reported, rescaled with the collision frequency ω_c, together with the parabolic fit via the formula $\gamma(k) = \gamma_b + \nu k^2$ (continuous red line).

the vorticity field. The behavior described above is in good agreement with experimental results obtained for driven granular fluids, as reported in [38] and, more recently, in [32].

From equation (19) we also find that the fluctuations decay exponentially

$$\langle u_\perp(k,t)u_\perp(-k,0)\rangle \sim S_\perp(k)\mathrm{e}^{-(\gamma_b+\nu k^2)t}, \tag{24}$$

with a characteristic time $\tau(k) = \gamma(k)^{-1} = (\gamma_b + \nu k^2)^{-1}$. Such a behavior is also observed for elastic fluids, with the only difference being that in that case $S_\perp(k) = T_b/n$ is constant. The length-scale $\xi = \sqrt{\nu/\gamma_b}$ can therefore always be connected to the dynamical properties of the system. What is peculiar for the out-of-equilibrium regime is that the so defined ξ also represents the extent of correlations of the vorticity field, thus establishing a remarkable link between static correlations and dynamical ones.

Figure 2 shows the correlators $C_\perp(k,t) = \langle u_\perp(k,t)u_\perp(-k,0)\rangle/\langle|u_\perp(k)|^2\rangle$ for different values of k and the same packing fraction as measured in numerical simulations. Let us notice that the decay of $\langle u_\perp(k,t)u_\perp(-k,0)\rangle$ is always exponential: we can therefore *a posteriori* support the validity of linear hydrodynamics, from which the Langevin equation for shear modes is obtained. By interpolating with a parabola the characteristic time $\tau(k)$ as a function of k, see the inset of figure 2, we obtain the shear viscosity ν. Let us stress the deep connection between statics and dynamics in the out-of-equilibrium regime: inserting the values of ν obtained from the dynamics into equation (21), we find curves that well superimpose the numerical data for $\langle u_\perp(k)u_\perp(-k)\rangle$ (see figure 3). The values of ν obtained from the dynamics of shear modes can be independently obtained as fitting parameters of $S_\perp(k)$ via equation (21). The values of ν obtained with the two different procedures are compatible, as can be seen from table 1. They are also reasonably close to the dense EHS predictions, presented in table 1.
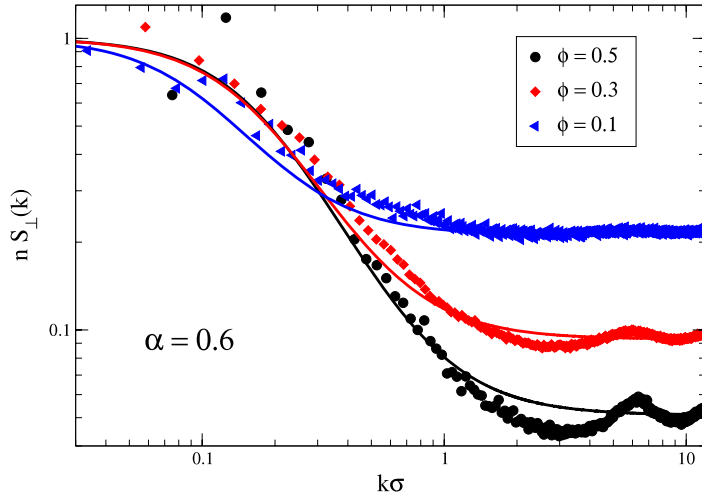
Figure 3. Shear mode structure factor $nS_\perp(k)$ at different packing fractions for $\alpha = 0.6$. The full curves are drawn by inserting into equation (21) the values of ν obtained from the decay of dynamical correlators.

Table 1. Comparison of the shear viscosity obtained from statics (fit via equation (21)), dynamics (fit via equation (24)) and the dense EHS approximation.

ϕ	Statics	Dynamics	Dense EHS
0.1	0.0062	0.0072	0.0111
0.2	0.0036	0.0041	0.0052
0.3	0.0025	0.0031	0.0039
0.4	0.0026	0.0027	0.0037
0.5	0.0020	0.0028	0.0041

3.2. Longitudinal modes

3.2.1. Static correlations. The same considerations discussed above for shear modes also hold for the other hydrodynamic modes, which are coupled to each other. In order to study their behavior we have to take into account all the elements of the dynamical matrix. In particular, the matrix of static structure factors $\mathbf{S}(\mathbf{k})$ with elements $S_{ab}(k)$ is obtained by solving the following linear system:

$$\mathbf{M}(k)\mathbf{S}(k) + \mathbf{S}^\dagger(k)\mathbf{M}^\dagger(k) + \mathbf{C}(k) = 0, \tag{25}$$

where the matrix of noises $\mathbf{C}(k)$ is such that

$$V^{-1}\langle \mathbf{f}(\mathbf{k}, t) \otimes \mathbf{f}(-\mathbf{k}, t') \rangle = \mathbf{C}(\mathbf{k})\delta(t - t'). \tag{26}$$

Here

$$\mathbf{C}(\mathbf{k}) = \mathrm{diag}\left[0, \frac{2T_g}{dn}(4T_b\gamma_b + 2D_T T_g k^2), \frac{2}{n}(T_b\gamma_b + \nu_l T_g k^2), \frac{2}{n}(T_b\gamma_b + \nu T_g k^2)\right], \tag{27}$$

where $\mathrm{diag}[x, y, z, w]$ denotes a diagonal matrix with elements x, y, z, w.
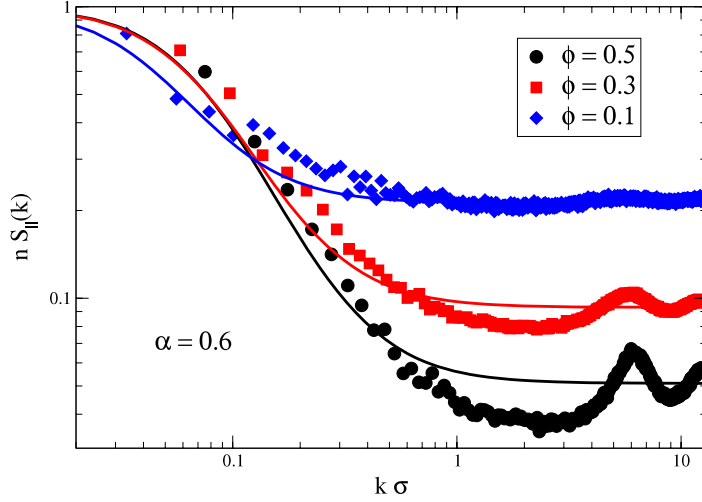
11

Figure 4. Longitudinal mode structure factor $nS_{\parallel}(k)$ at different packing fractions, for $\alpha = 0.6$. The full curves are drawn by inserting into equation (32) the values of ξ_{l}, defined in equation (31), obtained from best fits of the dynamical structure factors.

The expression of the longitudinal structure factor,

$$nS_{\parallel}(k) = N^{-1}\langle|u_{l}(k)|^{2}\rangle, \tag{28}$$

turns out to be the ratio between two even polynomial functions of the sixth order in k:

$$nS_{\parallel}(k) = \frac{S_{0} + S_{2}k^{2} + S_{4}k^{4} + S_{6}k^{6}}{S_{0}' + S_{2}'k^{2} + S_{4}'k^{4} + S_{6}'k^{6}}. \tag{29}$$

In the above expression eight constants have been introduced, which depend in a complicated manner on all the parameters of the system. Let us focus here on the asymptotic behavior of $S_{\parallel}(k)$ at large and small values of k. From equation (3) there follows the relation $d\gamma_{0}\omega_{c}/2 = \gamma_{b}(T_{b} - T_{g})/T_{g}$, which allows us to recast the series expansion around $k = 0$ of the expression in equation (29) in the form

$$nS_{\parallel}(k \to 0) \simeq T_{b} - (T_{b} - T_{g})\xi_{l}^{2}k^{2} + \mathcal{O}(k^{2}), \tag{30}$$

with

$$\xi_{l}^{2} = \frac{\nu_{l}^{*}}{\gamma_{b}} = \frac{1}{\gamma_{b}}\left[\nu_{l} + \frac{\gamma_{b}T_{b}}{nT_{g}(\gamma_{b} + \gamma_{0}\omega_{c})(2\gamma_{b} + 3\gamma_{0}\omega_{c})}\left(\frac{4p^{2}}{d^{2}nT_{g}} + \frac{2g(n)p}{3d}\right)\right]. \tag{31}$$

Up to $\mathcal{O}(k^{2})$ the expression in equation (30) is equivalent to

$$nS_{\parallel}(k) = T_{g} + \frac{(T_{b} - T_{g})}{1 + \xi_{l}^{2}k^{2}}, \tag{32}$$

namely a form analogous to the structure factor we found for the shear modes. In figure 4 we show the static structure factors for different packing fractions. Again, notice that in the limit $\gamma_{b} \to 0$ with $\gamma_{b}T_{b}$ finite the behavior $S_{\parallel}(k) \sim 1/k^{2}$ found in [18] is recovered. Albeit the above expression is in principle only valid for low k values, it captures also the

large k limit, when fine oscillations are disregarded. Indeed, expanding equation (29) for large k values we find

$$nS_\parallel(k \to \infty) \simeq T_\mathrm{g} + \frac{(T_\mathrm{b} - T_\mathrm{g})}{\xi_\mathrm{l}^2 k^2}. \tag{33}$$

Such a discussion shows that even for longitudinal modes the viscosity ν_l is related to a finite correlation length, measurable from static velocity correlations when the system is out of equilibrium with $T_\mathrm{g} < T_\mathrm{b}$. The behavior of that length when the packing fraction is increased will be discussed in section 4.

3.2.2. Dynamical correlations. Dynamical correlations for longitudinal modes are less simple than those for the shear mode, since they are given by a superposition of different (real and imaginary) exponentials. The dynamical structure factors are obtained by solving the equation of motion (10), which, in the frequency domain, reads as

$$\tilde{\mathbf{M}}(\mathbf{k},\omega)\delta\tilde{\mathbf{a}}(\mathbf{k},\omega) = \tilde{\mathbf{f}}(\mathbf{k},\omega), \tag{34}$$

where

$$\tilde{\mathbf{M}}(\mathbf{k},\omega) = \mathrm{i}\omega\mathbf{I} - \mathbf{M}(\mathbf{k}), \tag{35}$$

with $\mathbf{I}$ the identity matrix,

$$\delta\tilde{a}(\mathbf{k},\omega) = \int_{-\infty}^{\infty} \mathrm{d}t\, \delta a(\mathbf{k},t)\mathrm{e}^{-\mathrm{i}\omega t}, \tag{36}$$

and

$$V^{-1}\langle\tilde{\mathbf{f}}(\mathbf{k},\omega) \otimes \tilde{\mathbf{f}}(-\mathbf{k},\omega')\rangle = \mathbf{C}(\mathbf{k})\delta(\omega + \omega'), \tag{37}$$

$\mathbf{C}(k)$ being defined in equation (27). Multiplying equation (34) on the left by $\tilde{\mathbf{M}}^{-1}(k,\omega)$ and on the right by $\delta\tilde{\mathbf{a}}^\mathrm{T}(-k,-\omega)$ (where X^T denotes the transpose of X) and averaging over the noise, we obtain the matrix of dynamical structure factors

$$\mathbf{S}(k,\omega) = V^{-1}\langle\tilde{\mathbf{M}}^{-1}(k,\omega)\tilde{\mathbf{f}}(k)\delta\tilde{\mathbf{a}}^\mathrm{T}(-k,-\omega)\rangle = \tilde{\mathbf{M}}^{-1}(k,\omega)\mathbf{C}(k)[\tilde{\mathbf{M}}^\mathrm{T}(-k,-\omega)]^{-1}, \tag{38}$$

where in the last equality we have used the Hermitian conjugate of equation (34) and the relation (37).

The dynamical structure factors $S_{nn}(k,\omega)$ and $S_\parallel(k,\omega)$ take the explicit forms

$$
\begin{aligned}
S_{nn}(k,\omega) = n^2k^2(\{[\omega^2 + (2\gamma_\mathrm{b} + D_\mathrm{T}k^2 + 3\gamma_0\omega_\mathrm{c})^2]((2\gamma_\mathrm{b}T_\mathrm{b}/n) + (2\nu k^2 T_\mathrm{g}/n)) + k^2(p/nT_\mathrm{g})^2 \\
\times ((4D_\mathrm{T}T_\mathrm{g}^2k^2/nd) + (8T_\mathrm{g}\gamma_\mathrm{b}T_\mathrm{b}/nd))\}\{|\det\tilde{\mathbf{M}}|^2\}^{-1}),
\end{aligned} \tag{39}
$$

where

$$
\begin{aligned}
|\det\tilde{\mathbf{M}}|^2 = \Bigg[-\omega^2(3\gamma_0\omega_\mathrm{c} + D_\mathrm{T}k^2 + \nu k^2 + 3\gamma_\mathrm{b}) + k^2\Big((2\gamma_\mathrm{b} + 3\gamma_0\omega_\mathrm{c})v_\mathrm{T}^2 - \frac{g(n)p\gamma_0\omega_\mathrm{c}}{n} \\
+ v_\mathrm{T}^2 D_\mathrm{T}k^2\Big)\Bigg]^2 + \Bigg\{\omega^3 - \omega\Big[\gamma_\mathrm{b}(2\gamma_\mathrm{b} + 3\gamma_0\omega_\mathrm{c}) + k^2\Big(D_\mathrm{T}(\nu k^2 + \gamma_\mathrm{b}) + \nu(2\gamma_\mathrm{b} \\
+ 3\gamma_0\omega_\mathrm{c}) + \frac{2p^2}{dn^2 mT_\mathrm{g}} + v_\mathrm{T}^2\Big)\Big]\Bigg\}^2,
\end{aligned} \tag{40}
$$

Table 2. Comparison of the theoretical predictions of equations (3) and (A.2) and numerical results for T_g and ω_c.

	$\alpha = 0.6$		$\alpha = 0.8$	
	Sim	Dense EHS	Sim	Dense EHS
		$\phi = 0.5$		
T_g	0.051	0.0416	0.066	0.0603
ω_c	179	160	181	181
		$\phi = 0.3$		
T_g	0.093	0.0829	0.125	0.1185
ω_c	79	83	85	85
		$\phi = 0.1$		
T_g	0.212	0.2055	0.286	0.2820
ω_c	26	25	29	28

and

$$S_{\parallel}(k,\omega) = \frac{\omega^2}{n^2 k^2} S_{nn}(k,\omega). \tag{41}$$

All the coefficients appearing in these expressions can be evaluated within the dense EHS approximation, so that equation (41) can be used in order to obtain ν_l and D_T from the numerical data. Clearly the writing of physical quantities, such as $v_T^2 = (\partial p/\partial n)_T$ or p itself, with dense EHS formulas leads to systematic errors. The amplitude of this error can be estimated, for instance, by comparing the theoretical prediction of the dense EHS collision frequency with the collision frequency measured in simulations. In table 2 are listed both dense EHS and numerical collision frequencies at different packing fractions. Again it is found that the dense EHS prediction is quite good.

In order to obtain the longitudinal viscosity and the thermal diffusion coefficient, we fit our numerical data for the longitudinal modes using equation (41), where all parameters except ν_l and D_T are fixed to the dense EHS values and T_g is the one measured in simulations. In figure 5 $S_{\parallel}(k,\omega)$ is shown for different values of k and fixed $\phi = 0.5$, together with the best fit curves. The values of ν_l and D_T so obtained, together with those computed within the dense EHS approximation, for different values of ϕ and α, are reported in table 3 and within errors are found independent of k. This fact represents an *a posteriori* check that we are in the regime of validity of linearized hydrodynamics. Indeed, in equations (41) and (40) ν_l appears as a k-independent variable. Only at low packing fraction do we observe a dependence on k. This is perhaps due to diluteness, which implies too large a mean free path or mean free time with respect to mesoscopic scales.

In figure 6 we also show the time decay of the dynamical structure factor. One can appreciate, in the time domain, the superposition of different real and imaginary exponentials, which determines a mix of damping and propagation.

The dynamical structure factor at fixed k and different packing fractions is reported in figure 7: it is remarkable that we observe a time-scale, individuated by the peak frequency of $S_{\parallel}(k,\omega)$, which increases as the packing fraction is increased. Such behavior is consistent
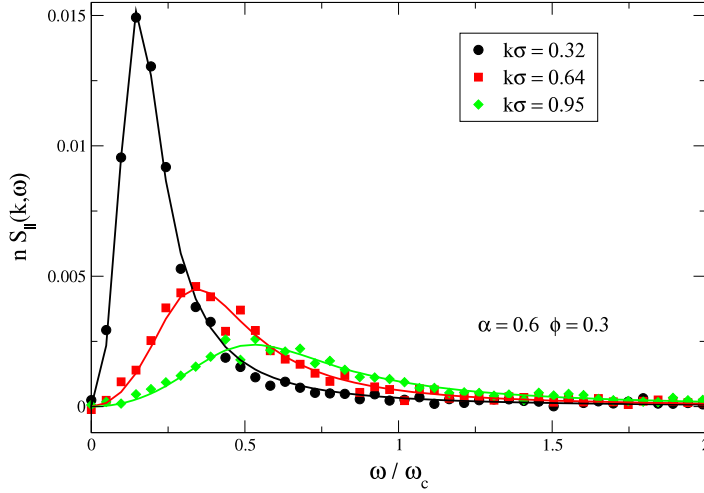
Figure 5. Dynamical structure factor $nS_{\parallel}(k,\omega)$ at fixed packing fractions ϕ and different momenta. Identifying a characteristic time τ_{peak} with the frequency of the maximum of the curve we see that $\tau_{\text{c}}/\tau_{\text{peak}} = \omega/\omega_{\text{c}}$ grows with the wavevector, namely longitudinal modes of higher momentum decay faster. The continuous lines show the best fit results via equation (41), with D_{T} and ν_{l} as fitting parameters and all other coefficients fixed with the dense EHS predictions.

with the observation, discussed in detail below, of a growth of the correlation lengths defined above, together with the packing fraction.

We conclude this section by stressing the remarkable agreement between numerical $S_{\parallel}(k)$ data and the expression of equation (32), see figure 4, with ν_{l} measured from dynamics and the renormalization term entering the definition of ν_{l}^{*} (see equation (31)) calculated within the dense EHS approximation and reported in table 3.

4. Summary and conclusions: transport coefficients and non-equilibrium correlation lengths

In conclusion, we have studied both static and dynamical correlations for hydrodynamic fluctuations of the velocity and density fields; indeed we recall equation (41) which gives a direct relation between the density and longitudinal velocity structure factors. A main comment concerns the good success of analytical predictions: comparison with simulations shows a fair agreement up to $\phi = 0.5$, with the values for most of the parameters directly given in the dense EHS approximation. This signals a success of the three main ingredients: (1) dense EHS theory for transport coefficients, working even at quite high densities, (2) scale separation and granular hydrodynamics, and (3) the prescription of equations (12)–(14) for the hydrodynamic noise. The last ingredient is perhaps the most interesting, if one considers how hard the characterization is in simple terms of non-equilibrium systems. Moreover, the assumption of white internal noise is less obvious than in the case of simple random kicks without drag [37]: in that case, the absence of drag ($\gamma_{\text{b}} = 0$) implies a relaxation time at large scales, $k \to 0$, which diverges, making a
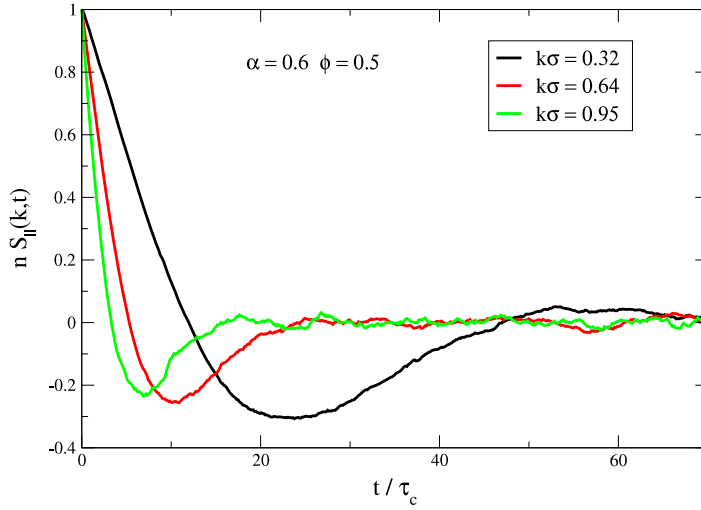
15

Figure 6. Dynamical structure factor $nS_\parallel(k,t)$ at fixed packing fraction ϕ and different momenta. The observed oscillations are in agreement with the eigenvalue spectrum in the interval of momenta considered: the eigenvalues of sound modes are complex conjugate, thus producing an oscillatory relaxation.

Table 3. Comparison of the theoretical predictions of equations (A.6)–(A.10) and fit results via equations (41) for D_T and ν_l.

	$\alpha = 0.6$		$\alpha = 0.8$	
	D_T	ν_l	D_T	ν_l
$\phi = 0.5$				
Fit results: $k\sigma = 0.5$	0.019	0.0053	0.020	0.011
$k\sigma = 0.6$	0.020	0.0046	0.018	0.011
$k\sigma = 0.8$	0.021	0.0055	0.019	0.0076
Dense EHS	0.018	0.0081	0.021	0.0090
$\phi = 0.3$				
Fit results: $k\sigma = 0.4$	0.017	0.0052	0.013	0.0098
$k\sigma = 0.5$	0.020	0.0058	0.013	0.0091
$k\sigma = 0.6$	0.017	0.0058	0.015	0.0079
Dense EHS	0.018	0.0057	0.021	0.0066
$\phi = 0.1$				
Fit results: $k\sigma = 0.2$	0.039	0.016	0.021	0.023
$k\sigma = 0.3$	0.028	0.016	0.019	0.018
$k\sigma = 0.4$	0.018	0.013	0.0096	0.016
Dense EHS	0.048	0.012	0.056	0.014

solid base for assuming the fast relaxation of noise due to microscopic degrees of freedom. In our model, in principle, the drag could be large enough to make even large scales fast, making it difficult to define hydrodynamic fields. Recent experiments show that, even if that could be a realistic situation, this does not change dramatically the qualitative behavior of the structure factors [32].
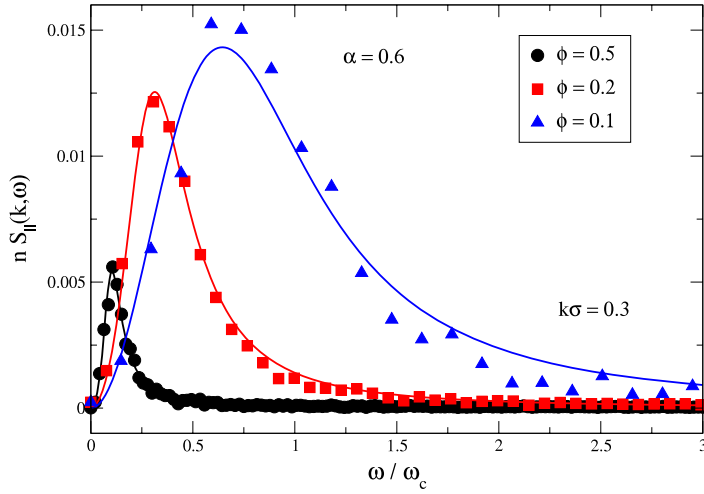
16

Figure 7. Dynamical structure factor $nS_\parallel(k,\omega)$ at fixed momentum k and different packing fractions. Identifying a characteristic time τ_{peak} with the frequency of the maximum of the curve we see that $\tau_{\text{c}}/\tau_{\text{peak}} = \omega/\omega_{\text{c}}$ grows when the packing fraction is lowered, namely the sound modes decay faster compared to the microscopic time-scale. The continuous lines show the best fit results via equation (41), with D_{T} and ν_{l} as fitting parameters and all other coefficients fixed with the dense EHS predictions.

One of the main results of our study is the presence of spatial order in the form of non-equilibrium velocity correlations. This should be related to the slowing down of the dynamics with increasing packing fraction in granular systems [39, 20], and with the existence of a time-scale growing with the density, as observed in [11]. As discussed in section 3, in our model the competition between different relaxation mechanisms given by the kinematic and longitudinal viscosities ν and ν_{l} and the thermostat damping γ_{b} gives rise to a couple of length-scales characterizing non-equilibrium structure factors: $\xi = \sqrt{\nu/\gamma_{\text{b}}}$ and $\xi_{\text{l}} = \sqrt{\nu_{\text{l}}^*/\gamma_{\text{b}}}$. The first trivial observation is that allowing $\gamma_{\text{b}} \to 0$ such lengths diverge. This means that, according to the prediction of [18], the largest-scale correlations are always equal to the size of the system, which is the largest size available. In our model there is a cut-off on such correlations imposed by the viscous drag $\gamma_{\text{b}} > 0$ due to the interaction with the thermal bath. The existence of such a cut-off, which represents a fixed parameter at different packing fractions, allows us to show that by increasing the packing fraction the extent of correlations is effectively increased. While the absolute value of ξ is only slightly enhanced when ϕ is increased, as also observed in experiments in [38], we stress that, in order to appreciate the physical meaning of such a length at different densities, one has to compare it with the microscopic relevant spatial scale in the system, which is given by the mean free path of the particles $\lambda_0 = \sqrt{\pi}\sigma/(8\phi\chi(\phi))$ and which also changes with the packing fraction. Then one finds that ξ/λ_0 is remarkably increased at high densities, as can be seen in figure 8, and also in recent experiments [32]. We may summarize the observed phenomenon by saying that the higher the packing fraction is the higher the number of intermediate scattering events between two different particles must be in order to decorrelate their velocities. This scenario could be reflected in transitions of dynamical origin, at higher packing fractions [40]–[42], [39].
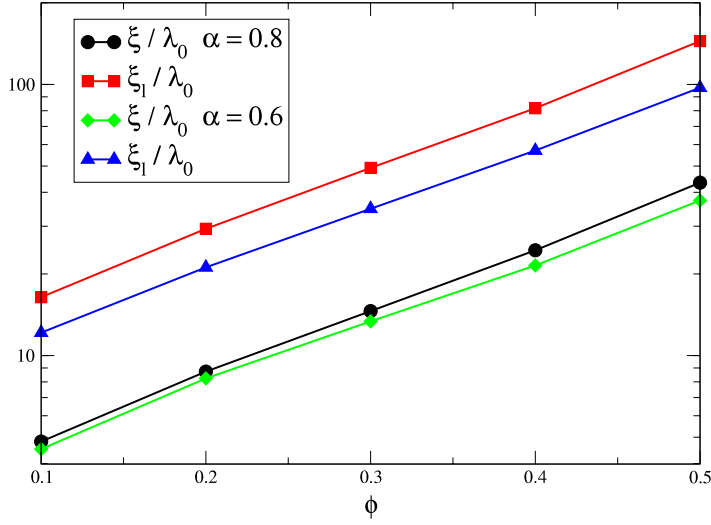
Figure 8. Correlation lengths ξ and ξ_l, rescaled with the mean free path λ_0, for different packing fractions and several values of the restitution coefficient. The extent of correlations grows exponentially with the packing fraction. Notice also that, at fixed ϕ, ξ and ξ_l are larger for higher values of α. However the amplitude of the correlations, ruled by $T_b - T_g$, is smaller, see equations (21) and (30).

Acknowledgments

Appendix A. Dense EHS formulas for hydrodynamic coefficients

The definitions of the parameters entering the matrix $\mathbf{M}$ are

$$v_T^2 = \left[\frac{\partial p}{\partial \rho}\right]_T, \tag{A.1}$$

$$\omega_c = \Omega_d \chi(\phi) n \sigma^{d-1} \sqrt{\frac{T_g}{\pi m}}, \tag{A.2}$$

$$g(\phi) = 2\left(1 + \frac{\phi}{\chi(\phi)}\frac{\partial \chi(\phi)}{\partial \phi}\right). \tag{A.3}$$

In the dense EHS approximation the pressure p can be written as

$$p(n) = nT_g\left(1 + \frac{\Omega_d \chi n \sigma^d}{2d}\frac{1+\alpha}{2}\right), \tag{A.4}$$

which in $d = 2$ reads as

$$p(\phi) = \frac{4}{\pi\sigma^2}\phi T_g(1 + \phi\chi(\phi)(1 + \alpha)), \tag{A.5}$$

where use has been made of the relation between packing fraction and density $n = 4\phi/(\pi\sigma^2)$, and of the definition $\Omega_{\mathrm{d}} = 2\pi^{d/2}/\Gamma(d/2)$ with $d = 2$. Notice also that we have taken into account the correction due to the inelasticity, as given in [43]. There are dense EHS formulas also for the dependence of the diffusion coefficients on the packing fraction and the granular temperature. In the following such formulas are written for a 2d system. In this case, we use the Verlet–Levesque approximation for the pair correlation function at contact: $\chi(\phi) = (1 - 7\phi/16)/(1 - \phi)^2$.

Shear viscosity:

$$\eta_E = \nu_0 \left[\frac{1}{\chi(\phi)} + 2\phi + \left(1 + \frac{8}{\pi}\right) \chi(\phi)\phi^2 \right], \tag{A.6}$$

with

$$\nu_0 = \frac{1}{2\sigma} \left(\frac{mT_{\mathrm{g}}}{\pi} \right)^{1/2}. \tag{A.7}$$

Bulk viscosity:

$$\zeta_E = \frac{8\phi^2\chi(\phi)}{\pi\sigma} \left(\frac{mT_{\mathrm{g}}}{\pi} \right)^{1/2}. \tag{A.8}$$

Thermal diffusivity:

$$\kappa_E = \kappa_0 \left[\frac{1}{\chi(\phi)} + 3\phi + \left(\frac{9}{4} + \frac{4}{\pi}\right) \chi(\phi)\phi^2 \right], \tag{A.9}$$

with

$$\kappa_0 = \frac{2}{\sigma} \left(\frac{T_{\mathrm{g}}}{\pi m} \right)^{1/2}. \tag{A.10}$$

Appendix B. Noises

In this appendix we present a detailed discussion of the noise terms appearing in the fluctuating hydrodynamic equations (10). Let us start from the external noises, which can be simply obtained from equations (2) and (4). We find that the noise contributions to the equations for the velocity and temperature fields are, respectively,

$$\boldsymbol{\xi}^{\mathrm{ex}}(\mathbf{r}, t) = \frac{1}{n} \sum_i \boldsymbol{\xi}_{\mathrm{b},i}(t)\delta(\mathbf{r} - \mathbf{r}_i(t)), \tag{B.1}$$

$$\theta^{\mathrm{ex}}(\mathbf{r}, t) = \frac{2m}{dn} \sum_i \mathbf{v}_i(t) \cdot \boldsymbol{\xi}_{\mathrm{b},i}(t)\delta(\mathbf{r} - \mathbf{r}_i(t)). \tag{B.2}$$

These are Gaussian noises with variances

$$\langle \xi_\alpha^{\mathrm{ex}}(\mathbf{r}, t)\xi_\beta^{\mathrm{ex}}(\mathbf{r}', t')\rangle = \frac{1}{n} \frac{2\gamma_{\mathrm{b}} T_{\mathrm{b}}}{m} \delta_{\alpha\beta}\delta(t - t')\delta(\mathbf{r} - \mathbf{r}'),$$

$$\langle \theta^{\mathrm{ex}}(\mathbf{r}, t)\theta^{\mathrm{ex}}(\mathbf{r}', t')\rangle = \frac{4mT_{\mathrm{g}}}{dn} \frac{2\gamma_{\mathrm{b}} T_{\mathrm{b}}}{m} \delta(t - t')\delta(\mathbf{r} - \mathbf{r}'). \tag{B.3}$$

In order to describe the local spontaneous microscopic fluctuations of the fluid, we also include in our description internal conserved Gaussian noises $\boldsymbol{\theta}^{\mathrm{in}}$ and $\boldsymbol{\xi}^{\mathrm{in}}$, which enter the constitutive equations for $\mathbf{J}$ and $\boldsymbol{\Pi}$, respectively,

$$\mathbf{J} = -\kappa \boldsymbol{\nabla} T + \boldsymbol{\theta}^{\mathrm{in}}, \tag{B.4}$$

$$\boldsymbol{\Pi} = p\mathbf{1} - \eta[\boldsymbol{\nabla}\mathbf{u} + (\boldsymbol{\nabla}\mathbf{u})^{\dagger}] + \left(\frac{2}{d}\eta - \zeta\right)\mathbf{1}\boldsymbol{\nabla}\cdot\mathbf{u} + \boldsymbol{\xi}^{\mathrm{in}}, \tag{B.5}$$

where κ is the heat conductivity, p is the local pressure, $\mathbf{1}$ is the unit tensor, η is the shear viscosity and ζ is the bulk viscosity. The amplitudes of such noises are obtained from the fluctuation-dissipation theorem [4, 5, 44]

$$\langle \xi_{\alpha\beta}^{\mathrm{in}}(\mathbf{r},t)\xi_{\gamma\delta}^{\mathrm{in}}(\mathbf{r}',t')\rangle = 2T_{\mathrm{g}}[\eta(\delta_{\alpha\gamma}\delta_{\beta\delta} + \delta_{\alpha\delta}\delta_{\beta\gamma}) + \left(\zeta - \frac{2}{d}\eta\right)\delta_{\alpha\beta}\delta_{\gamma\delta}]\delta(t-t')\delta(\mathbf{r}-\mathbf{r}'),$$
$$\langle \theta_{\alpha}^{\mathrm{in}}(\mathbf{r},t)\theta_{\beta}^{\mathrm{in}}(\mathbf{r}',t')\rangle = 2\kappa T_{\mathrm{g}}^2\delta_{\alpha\beta}\delta(t-t')\delta(\mathbf{r}-\mathbf{r}'). \tag{B.6}$$

Notice that, for granular systems, equation (B.4) should be modified, adding the term $-\mu\nabla n$ on the rhs, which takes into account the contribution to the heat current due to density gradients [45]. However, the transport coefficient μ is very small for driven systems [46], and therefore we have neglected this contribution.

Linearization

In order to obtain the linear approximation of the hydrodynamic equations, we consider how a homogeneous fluctuation of the temperature relaxes around its stationary value T_{g}. Therefore we start by linearizing equation (5) around T_{g}, with $n(\mathbf{r},t) = n$, $\mathbf{u} = 0$, $T(\mathbf{r},t) = T(t)$, and obtain

$$\delta\dot{T}(t) = -(2\gamma_{\mathrm{b}}/m + 3\gamma_0\omega_{\mathrm{c}})\delta T(t). \tag{B.7}$$

Notice that the quantity $-(2\gamma_{\mathrm{b}}/m + 3\gamma_0\omega_{\mathrm{c}})$ coincides with the heat mode eigenvalue $\lambda_{\mathrm{H}}(k=0)$.

Next, taking the linear terms around the non-equilibrium steady state in equations (5), introducing the external noises (B.1) and (B.2), and using equations (B.4) and (B.5), we obtain

$$\partial_{\mathrm{t}}\delta n(\mathbf{r},t) = -n\boldsymbol{\nabla}\cdot\mathbf{u}(\mathbf{r},t),$$

$$\partial_{\mathrm{t}}\mathbf{u}(\mathbf{r},t) = -\frac{1}{\rho}\boldsymbol{\nabla}p(\mathbf{r},t) + \nu\nabla^2\mathbf{u}(\mathbf{r},t) + (\nu_{\mathrm{l}} - \nu)\boldsymbol{\nabla}\boldsymbol{\nabla}\cdot\mathbf{u}(\mathbf{r},t)$$
$$\qquad - \frac{\gamma_{\mathrm{b}}}{m}\mathbf{u}(\mathbf{r},t) - \frac{1}{\rho}\boldsymbol{\nabla}\cdot\boldsymbol{\xi}^{\mathrm{in}}(\mathbf{r},t) + \boldsymbol{\xi}^{\mathrm{ex}}(\mathbf{r},t), \tag{B.8}$$

$$\partial_{\mathrm{t}}\delta T(\mathbf{r},t) = \frac{2\kappa}{nd}\nabla^2\delta T(\mathbf{r},t) - \frac{2p}{nd}\boldsymbol{\nabla}\cdot\mathbf{u}(\mathbf{r},t) - \frac{\gamma_0\omega_{\mathrm{c}}g(n)T_{\mathrm{g}}}{n}\delta n$$
$$\qquad - 2\frac{\gamma_{\mathrm{b}}}{m}\delta T(\mathbf{r},t) - 3\gamma_0\omega_{\mathrm{c}}\,\delta T(\mathbf{r},t) - \frac{2}{nd}\boldsymbol{\nabla}\cdot\boldsymbol{\theta}^{\mathrm{in}}(\mathbf{r},t) + \theta^{\mathrm{ex}}(\mathbf{r},t),$$

with $\rho\nu = \eta$

The velocity field $\mathbf{u}$ can be split into longitudinal and transverse components $\mathbf{u} = \mathbf{u}_{\mathrm{l}} + \mathbf{u}_{\perp}$, where $\boldsymbol{\nabla}\cdot\mathbf{u}_{\perp} = 0$ and $\boldsymbol{\nabla}\wedge\mathbf{u}_{\parallel} = 0$. With such a decomposition equations (B.8)

can be written

$$\partial_t \delta n(\mathbf{r}, t) = -n \boldsymbol{\nabla} \cdot \mathbf{u}(\mathbf{r}, t),$$

$$\partial_t \mathbf{u}_l(\mathbf{r}, t) = -\frac{1}{\rho} \boldsymbol{\nabla} p(\mathbf{r}, t) + \nu_l \boldsymbol{\nabla} \boldsymbol{\nabla} \cdot \mathbf{u}_l(\mathbf{r}, t) - \frac{\gamma_b}{m} \mathbf{u}_l(\mathbf{r}, t) - \frac{1}{\rho} \boldsymbol{\nabla} \cdot \boldsymbol{\xi}_l^{\mathrm{in}}(\mathbf{r}, t) + \boldsymbol{\xi}_l^{\mathrm{ex}}(\mathbf{r}, t),$$

$$\partial_t \mathbf{u}_\perp(\mathbf{r}, t) = \nu \nabla^2 \mathbf{u}_\perp(\mathbf{r}, t) - \frac{\gamma_b}{m} \mathbf{u}_\perp(\mathbf{r}, t) - \frac{1}{\rho} \boldsymbol{\nabla} \cdot \boldsymbol{\xi}_\perp^{\mathrm{in}}(\mathbf{r}, t) + \boldsymbol{\xi}_\perp^{\mathrm{ex}}(\mathbf{r}, t), \qquad \text{(B.9)}$$

$$\partial_t \delta T(\mathbf{r}, t) = \frac{2\kappa}{nd} \nabla^2 \delta T(\mathbf{r}, t) - \frac{2p}{nd} \boldsymbol{\nabla} \cdot \mathbf{u}(\mathbf{r}, t) - 2\frac{\gamma_b}{m} \delta T(\mathbf{r}, t) - 3\gamma_0 \omega_c \ \delta T(\mathbf{r}, t)$$
$$- \frac{\gamma_0 \omega_c g(n) T_g}{n} \delta n - \frac{2}{nd} \boldsymbol{\nabla} \cdot \boldsymbol{\theta}^{\mathrm{in}}(\mathbf{r}, t) + \theta^{\mathrm{ex}}(\mathbf{r}, t),$$

where

$$\langle \xi_{\perp,\alpha\beta}^{\mathrm{in}}(\mathbf{r}, t) \xi_{\perp,\gamma\delta}^{\mathrm{in}}(\mathbf{r}', t') \rangle = 2T_g \eta (\delta_{\alpha\gamma}\delta_{\beta\delta} + \delta_{\alpha\delta}\delta_{\beta\gamma} - 2\delta_{\alpha\beta}\delta_{\gamma\delta}) \delta(t - t') \delta(\mathbf{r} - \mathbf{r}'),$$

$$\langle \xi_{l,\alpha\beta}^{\mathrm{in}}(\mathbf{r}, t) \xi_{l,\gamma\delta}^{\mathrm{in}}(\mathbf{r}', t') \rangle = 2T_g \left[\zeta + \frac{2\eta(d-1)}{d} \right] \delta_{\alpha\beta}\delta_{\gamma\delta} \delta(t - t') \delta(\mathbf{r} - \mathbf{r}'), \qquad \text{(B.10)}$$

and

$$\langle \xi_\perp^{\mathrm{ex}}(\mathbf{r}, t) \xi_\perp^{\mathrm{ex}}(\mathbf{r}', t') \rangle = \langle \xi_l^{\mathrm{ex}}(\mathbf{r}, t) \xi_l^{\mathrm{ex}}(\mathbf{r}', t') \rangle = \frac{1}{n} \frac{2\gamma_b T_b}{m} \delta(t - t') \delta(\mathbf{r} - \mathbf{r}'). \qquad \text{(B.11)}$$

Finally, taking the Fourier transform of equations (B.9)–(B.11) we obtain equation (10) and what follows.

References

[1] Jaeger H M, Nagel S R and Behringer R P, *Granular solids, liquids, and gases*, 1996 *Rev. Mod. Phys.* **68** 1259

[2] Pöschel T and Luding S (ed), 2001 *Granular Gases* (*Springer Lecture Notes in Physics* vol 564) (Berlin: Springer)

[3] Pöschel T and Schwager T, 2005 *Computational Granular Dynamics* (Berlin: Springer)

[4] Landau L D and Lifchitz E M, 1967 *Physique Statistique* Éditions MIR

[5] Fox R F and Uhlenbeck G E, *Contributions to non-equilibrium thermodynamics. I. Theory of hydrodynamical fluctuations*, 1970 *Phys. Fluids* **13** 1893

[6] Ortiz de Zárate J M and Sengers J V, 2006 *Hydrodynamic Fluctuations in Fluids and Fluid Mixtures* (Amsterdam: Elsevier)

[7] Sengers J V and Ortiz de Zárate J M, *Velocity fluctuations in laminar fluid flow*, 2010 *J. Non-Newton. Fluid Mech.* **165** 925

[8] Puglisi A, Baldassarri A and Vulpiani A, *Violations of the Einstein relation in granular fluids: the role of correlations*, 2007 *J. Stat. Mech.* P08016

[9] Brey J J, Garcia de Soria M I and Maynar P, *Breakdown of the fluctuation-dissipation relations in granular gases*, 2008 *Europhys. Lett.* **84** 24002

[10] Villamaina D, Puglisi A and Vulpiani A, *The fluctuation-dissipation relation in sub-diffusive systems: the case of granular single-file diffusion*, 2008 *J. Stat. Mech.* L10001

[11] Sarracino A, Villamaina D, Gradenigo G and Puglisi A, *Irreversible dynamics of a massive intruder in dense granular fluids*, 2010 *Europhys. Lett.* **92** 34001

[12] Puglisi A, Baldassarri A and Loreto V, *Fluctuation-dissipation relations in driven granular gases*, 2002 *Phys. Rev.* E **66** 061305

[13] Garzó V, *On the Einstein relation in a heated granular gas*, 2004 *Physica A* **343** 105

[14] Sarracino A, Villamaina D, Costantini G and Puglisi A, *Granular brownian motion*, 2010 *J. Stat. Mech.* P04013

[15] D'Anna G, Mayor P, Gremaud G, Barrat A, Loreto V and Nori F, *Observing brownian motion in vibration-fluidized granular matter*, 2003 *Nature* **424** 909

[16] Baldassarri A, Barrat A, D'Anna G, Loreto V, Mayor P and Puglisi A, *What is the temperature of a granular medium?*, 2005 *J. Phys.: Condens. Matter* **17** S2405

[17] Williams D R M and MacKintosh F C, *Driven granular media in one dimension: correlations and equation of state*, 1996 *Phys. Rev.* E **54** R9

[18] van Noije T P C, Ernst M H, Trizac E and Pagonabarraga I, *Randomly driven granular fluids: large-scale structure*, 1999 *Phys. Rev.* E **59** 4326

[19] Puglisi A, Loreto V, Marconi U M B, Petri A and Vulpiani A, *Clustering and non-Gaussian behavior in granular matter*, 1998 *Phys. Rev. Lett.* **81** 3848

[20] Vollmayr-Lee K, Aspelmeier T and Zippelius A, *Hydrodynamic correlation functions of a driven granular fluid in steady state*, 2011 *Phys. Rev.* E **83** 001301

[21] Luding S, *Molecular dynamics simulations of granular materials, in the physics of granular media*, 2005 *The Physics of Granular Media* ed H Hinrichsen and D E Wolf (Weinheim: Wiley-VCH)

[22] Foster D, 1975 *Hydrodynamic Fluctuations, Broken Symmetry, and Correlation Functions* (Boulder, CO: Westview Press)

[23] Grossman E L, Zhou T and Ben-Naim E, *Towards granular hydrodynamics in two-dimensions*, 1997 *Phys. Rev.* E **55** 4200

[24] Brey J J, Dufty J W, Kim C S and Santos A, *Hydrodynamics for granular flow at low density*, 1998 *Phys. Rev.* E **58** 4638

[25] van Noije T P C, Ernst M H, Brito R and Orza J A G, *Mesoscopic theory of granular fluids*, 1997 *Phys. Rev. Lett.* **79** 411

[26] Goldhirsch I, *Scales and kinetics of granular flows*, 1999 *Chaos* **9** 659

[27] Kadanoff L P, *Built upon sand: theoretical ideas inspired by granular flows*, 1999 *Rev. Mod. Phys.* **71** 435

[28] Puglisi A, Cecconi F and Vulpiani A, *Models of fluidized granular materials: examples of non-equilibrium stationary states*, 2005 *J. Phys.: Condens. Matter* **17** S2715

[29] He X, Meerson B and Doolen G, *Hydrodynamics of thermal granular convection*, 2002 *Phys. Rev.* E **65** 030301(R)

[30] Brilliantov N V and Poschel T, *Self-diffusion in granular gases: Green–Kubo versus Chapman–Enskog*, 2005 *Chaos* **15** 026108

[31] Puglisi A, Assaf M, Fouxon I and Meerson B, *Attempted density blowup in a freely cooling dilute granular gas: hydrodynamics versus molecular dynamics*, 2008 *Phys. Rev.* E **77** 021305

[32] Gradenigo G, Sarracino A, Villamaina D and Puglisi A, *Non-equilibrium length in granular fluids: from experiment to fluctuating hydrodynamics*, 2011 arXiv:1103.0166

[33] Chapman S and Cowling T G, 1970 *The Mathematical Theory of Non-uniform Gases* (Cambridge: Cambridge University Press)

[34] García-Rojo R, Luding S and Brey J J, *Transport coefficients for dense hard-disk systems*, 2006 *Phys. Rev.* E **74** 061305

[35] Brey J J, Maynar P and Garcia de Soria M I, *Fluctuating hydrodynamics for dilute granular gases*, 2009 *Phys. Rev.* E **79** 051305

[36] Brey J J, Maynar P and Garcia de Soria M I, *Fluctuating Navier–Stokes equations for inelastic hard spheres or disks*, 2011 *Phys. Rev.* E **83** 041303

[37] Maynar P, de Soria M I G and Trizac E, *Fluctuating hydrodynamics for driven granular gases*, 2009 *Eur. Phys. J. Special Top.* **179** 123

[38] Prevost A, Egolf D A and Urbach J S, *Forcing and velocity correlations in a vibrated granular monolayer*, 2002 *Phys. Rev. Lett.* **89** 084301

[39] Kranz W T, Sperl M and Zippelius A, *Glass transition for driven granular fluids*, 2010 *Phys. Rev. Lett.* **104** 225701

[40] Olafsen J S and Urbach J S, *Two-dimensional melting far from equilibrium in a granular monolayer*, 2005 *Phys. Rev. Lett.* **95** 098002

[41] Reis P M, Ingale R A and Shattuck M D, *Crystallization of a quasi-two-dimensional granular fluid*, 2006 *Phys. Rev. Lett.* **96** 258001

[42] Watanabe K and Tanaka H, *Direct observation of medium-range crystalline order in granular liquids near the glass transition*, 2008 *Phys. Rev. Lett.* **100** 158002

[43] Pagonabarraga I, Trizac E, van Noije T P C and Ernst M H, *Randomly driven granular fluids: collisional statistics and short scale structure*, 2001 *Phys. Rev.* E **65** 011303

[44] Marini Bettolo Marconi U, Puglisi A, Rondoni L and Vulpiani A, *Fluctuation-dissipation: response theory in statistical physics*, 2008 *Phys. Rep.* **461** 111

[45] Jenkins J T and Richman M W, *Kinetic theory for plane flows of a dense gas of identical, rough, inelastic, circular disks*, 1985 *Phys. Fluids* **28** 3485

[46] Garzó V and Montanero J M, *Transport coefficients of a heated granular gas*, 2002 *Physica* A **313** 336